CRYOSORPTION OF HYDROGEN BY 12-20°K CARBON DIOXIDE CRYODEPOSITS

R. Dawbarn

ARO, Inc.

July 1967

AEROSPACE ENVIRONMENTAL FACILITY
ARNOLD ENGINEERING DEVELOPMENT CENTER
AIR FORCE SYSTEMS COMMAND
ARNOLD AIR FORCE STATION, TENNESSEE

NOTICES

When U. S. Government drawings specifications, or other data are used for any purpose other than a definitely related Government procurement operation, the Government thereby incurs no responsibility nor any obligation whatsoever, and the fact that the Government may have formulated, furnished, or in any way supplied the said drawings, specifications, or other data, is not to be regarded by implication or otherwise, or in any manner licensing the holder or any other person or corporation, or conveying any rights or permission to manufacture, use, or sell any patented invention that may in any way be related thereto.

Qualified users may obtain copies of this report from the Defense Documentation Center.

References to named commercial products in this report are not to be considered in any sense as an endorsement of the product by the United States Air Force or the Government.

CRYOSORPTION OF HYDROGEN BY 12-20°K CARBON DIOXIDE CRYODEPOSITS

R. Dawbarn
ARO, Inc.

AF - AEDC
Arnold AFS Tenn

FOREWORD

The research presented herein was sponsored by Arnold Engineering Development Center (AEDC), Air Force Systems Command (AFSC), Arnold Air Force Station, Tennessee, under Program Element 65402234.

The results of research reported herein were obtained by ARO, Inc. (a subsidiary of Sverdrup & Parcel and Associates, Inc.), contract operator of AEDC under Contract AF 40(600)-1200. The research was conducted in the Aerospace Environmental Facility (AEF) (AEDC) under ARO Project No. SW2705, and the manuscript was submitted for publication on May 22, 1967.

This technical report has been reviewed and is approved.

Paul L. Landry
Major, USAF
AF Representative, AEF
Directorate of Test

Leonard T. Glaser
Colonel, USAF
Director of Test

ABSTRACT

Carbon dioxide cryodeposits were investigated to determine their ability to sorb H_2. Various thicknesses from 5×10^{-5} to 1×10^{-3} cm were used, at temperatures of 12, 16, and 20°K. Pumping speeds of 28, 19, and 14 ℓ/sec-cm^2 were measured for the respective temperatures. An arbitrary "capacity" of the CO_2 cryodeposit for H_2 was defined. Within the limits of the experimental parameters varied, this capacity was found to be a direct function of the thickness of the cryodeposit and increased logarithmically as the temperature was lowered. No cryopumping of H_2 was observed with cryodeposits above 25°K. The CO_2 cryodeposits were readily contaminated by N_2, and the H_2 pumping speed dropped when N_2 was flowed in simultaneously with the H_2.

CONTENTS

TABLES

APPENDIX

Illustrations

NOMENCLATURE

K	Conductance of orifice in shroud, ℓ/sec
k	Conductance of leak, ℓ/sec
P	Pressure, mm Hg
R	Universal gas constant, ergs/mole-°K
S	Pumping speed, ℓ/sec
T	Temperature, °K
t	Time, sec
V	Volume, ℓ
ξ	Outgassing rate, ℓ/sec
σ	Gage calibration factor, mm Hg/division

SUBSCRIPTS

c	Inside shroud inside vacuum chamber
f	Gas addition system
ms	Mass spectrometer
n	Gage scale
o	Outside shroud but inside vacuum chamber

SECTION I
INTRODUCTION

Of the available methods of producing a vacuum environment, cryopumping offers the most promising means of producing a clean vacuum with exceptionally high pumping speeds. Unlike conventional cold trapped diffusion pumps, cryopumping is not limited by the conductance of the orifice leading to the pump. Since cryopanels can be built within the vacuum cell, their size is limited only by the size of the chamber and the quantity of cryogenic refrigerant available. The common atmospheric gases (N_2, O_2, CO_2, H_2O, A) are condensable on 20°K surfaces with vapor pressures below 10^{-11} mm. Hydrogen (H_2) and helium (He), although not major constituents of the atmosphere, are used extensively in aerospace technology.

Frequently, it is necessary to remove one or both of these noncondensible gases from a vacuum chamber with a system having a high pumping speed, while still maintaining a clean vacuum. If the liquid-helium (LHe)-cooled panels are available, H_2 may be cryopumped directly since its vapor pressure is about 10^{-7} torr at 4.2°K. Super-cooled He has been used by Chubb et al. to improve pumping speed and reduce the base pressure still further (Ref. 1).

Helium cannot be practically cryopumped since cryosurfaces on the order of 0.4°K are required for vapor pressures of 10^{-7} torr. However, some work has been done in this laboratory investigating the feasibility of pumping He by sorption on cryodeposits of A, N_2, and O_2. Although there was no measurable pumping above 5°K, pumping speeds as high as 50 percent of the theoretical maximum were obtained at 4.2°K (Ref. 2).

In many instances, LHe is not available or not feasible in the quantities required to pump large systems. However, many large aerospace chambers have GHe refrigerators capable of operating relatively large cryoarrays in the temperature range from 12 to 20°K. Several methods of sorbing H_2 have been found, although efforts to find sorbents among molecular sieves and cryodeposits that would provide a practical method of pumping He in this temperature range have so far been unsuccessful. Southerlan (Ref. 3) reports successful pumping of H_2 by H_2O cryodeposits at 20°K. Busol and Yuferov present data for CO_2 cryodeposits at 20°K and suggest that acetone, gasoline, and alcohol condensed at 20°K will also sorb H_2 but not as effectively as CO_2 (Ref. 4). Using O_2 and N_2 as cryodeposits at 20°K, Hemstreet et al. found no significant pumping of H_2; however, they report favorably on Molecular Sieve #5A cooled to 20°K (Ref. 5).

The experiments reported herein were centered on the ability of CO_2 cryodeposits to sorb H_2. The three questions to be investigated were: (1) the effect of thickness of the CO_2 cryodeposit, (2) the effect of temperature of the CO_2, and (3) the results of the CO_2-coated cryopanel pumping a mixture of H_2 and N_2.

SECTION II
APPARATUS

The chamber used in this study is shown in Fig. 1. It consists essentially of a 36-in. -high by 30-in. -diam vacuum chamber containing a 7-in. -diam spherical cryosurface and two independent gas addition systems. The vacuum chamber is constructed of stainless steel, all heliarc welded. A 25-in. -high by 24-in. -diam inner shroud of 1/8-in. copper can be cooled by circulating LN_2 through tubing welded to its outer surfaces. The cryosphere is centrally located inside the shroud, and its fill and vent lines are vacuum jacketed and shielded inside the chamber. The surface area of the sphere, available for pumping, is 970 cm^2.

There are two gas addition systems, one to add H_2 and the other to add CO_2. The gas addition systems (Fig. 2) are similar, each consisting of a surge tank, a pressure gage for measuring the fore-pressure of the gas, and a series of sintered stainless steel leaks arranged in parallel (Ref. 6). Gas flows from 5×10^{-2} to 5×10^{-7} torr-ℓ/sec can be metered into the chamber. Each gas addition system has an independent pumping station.

A thin-walled circular orifice in the bottom of the shroud provides a convenient method for frequent in-place calibration of the gages and mass spectrometer (see Section IV). The pressure in the working volume of the chamber is monitored by an ion gage and a mass spectrometer. Tubulation inside the chamber prevents the gages from directly sensing either the cryosurface or the calibration orifice. The time constant of the tubulation is calculated as 3.8×10^{-6} sec for H_2 at 300°K, and thus the response is much faster than any pressure changes to be followed in these experiments. A second ion gage, located on the outside wall of the chamber, is used to read the pressure on the far side of the orifice.

The vacuum chamber pumping system consists of a 6-in. oil diffusion pump with a LN_2 baffle. The diffusion pump is backed by a mechanical roughing pump. The chamber can be isolated from the

pumping system by a 6-in. high vacuum, gate valve. The entire vacuum system is equipped with outgassing heaters capable of producing chamber temperatures up to 500°K.

The cryosphere was plumbed directly to a He refrigerator (180-w cryostat), via vacuum jacketed transfer lines. An adjustable needle valve, located in the cryostat, was used to set the GHe flow. Temperatures in the sphere were indicated by a H_2 vapor pressure thermometer centered in the cryosphere.

SECTION III
PROCEDURE

With the chamber pumped down to its base operating pressure (10^{-8} torr), the refrigeration He was cycled through the cryosphere. The temperature was monitored by the H_2 vapor pressure thermometer in the sphere, and the inlet and outlet temperatures at the refrigerator were also recorded. By adjusting the bypass valve at the refrigerator, the cryosphere was stabilized at the required temperature. The temperature as recorded by the vapor pressure thermometer in the cryosphere agreed within 1°K of the mean of the input-output temperatures at the cryostat.

Following the procedure outlined in Section IV, the mass spectrometer and ion gage were calibrated for H_2 by flowing gas into the chamber through a previously measured leak.

After calibration, the H_2 flow was stopped and the chamber pumped to its base pressure (approximately 5×10^{-9} torr). At this point, the diffusion pump was valved off and the CO_2 admitted to the chamber through its gas addition system to precoat the sphere. The thin layers of CO_2 were formed by adding CO_2 to the chamber for a known time while a constant forepressure was maintained on the calibrated leak. Since it would have taken an excessively long time to use this same method for forming the thicker layers, the following technique was used. The CO_2 was bled into the surge tank to raise the pressure to the 300-mm range; then the surge tank system was closed, and the pressure recorded. The valve to the chamber was then slightly opened, and the pressure drop in the surge tank monitored. Chamber pressures below 50 μ were maintained during these additions. When the surge tank pressure had dropped to the desired level, the valve to the chamber was closed. From the volume of the surge tank system, the initial and final pressure, the total quantity of CO_2 admitted was calculated. The heat load from this gas addition caused a slight rise in the cryosphere temperature. The total cryodeposit was cooled to the required test temperature after the gas flow was shut off.

The H_2 was admitted to the chamber through its gas addition system for a measured interval and then shut off. A record of the resulting pressure rise and drop was made from the mass spectrometer trace. The additions of H_2 were repeated until the partial pressure of H_2 rose too high to be further monitored by the mass spectrometer. For the thicker deposits of CO_2, the H_2 was added at higher rates so that the CO_2 could be saturated in the time available.

The following tests were made since anticipated user tests would require a pump capable of removing a mixture of H_2 and N_2, and Busol et al. had reported that N_2 cryodeposits would not sorb H_2 (Ref. 4). The sphere was precoated with CO_2, and the chamber was then valved closed. The CO_2 gas addition system was pumped out and flushed with N_2. Hydrogen was then admitted to the chamber via a known leak and the pumping speed of the CO_2 cryodeposit recorded by noting the equilibrium H_2 partial pressure. The valve to the N_2 system was opened and N_2 admitted simultaneously.

The H_2 pumping speed of the CO_2 cryodeposit immediately started to deteriorate as evidenced by the slow rise in H_2 partial pressure. The N_2 flow was interrupted, and again the H_2 equilibrium partial pressure was recorded.

This procedure was repeated for several different N_2 flow rates. Each successive N_2 addition caused a decrease in the H_2 pumping speed of the CO_2 cryodeposit.

SECTION IV
CALIBRATION

4.1 LEAKS

Each leak was calibrated for the gases used, by recording the pressure drop in a known volume, as the gas flowed from this volume through the leak into the vacuum chamber (Ref. 2). Consider two volumes at pressures P_f and P_c, respectively, connected by a small leak with a conductance k. The resulting gas flow through the leak may be expressed as

$$V_f \frac{dP_f}{dt} = k\ (P_f - P_c)$$

If the pressure P_c is kept much lower than P_f by a pumping system, then the expression may be written

$$V_f \frac{dP_f}{dt} = k\, P_f$$

and

$$\frac{dP_f}{P_f} = \frac{k}{V_f}\, dt$$

Integration yields

$$ln\, P_f = \frac{k}{V_f}\, t + ln\, C$$

Using the initial conditions, $t = 0$, $P_f = P_i$. Then

$$ln\, \frac{P_f}{P_i} = \frac{kt}{V_f}$$

Thus, the conductance of the leak is given by

$$k = \frac{V_f}{t}\, ln\, \frac{P_f}{P_i}$$

The known volume, V_f, was measured by filling the components of the system with alcohol and measuring each volume during assembly. The pressure-time response during calibration was measured with a calibrated pressure transducer.

4.2 PUMP ORIFICE AND GAGE CALIBRATION

The vacuum system was pumped down with the diffusion pump, and the shroud was cooled to 77°K. The base pressure was measured by the ion gages. The pump was then closed off with the 6-in. gate valve, and the rate of rise caused by outgassing was recorded.

Using the previously calibrated leak, H_2 was admitted to the chamber at a known rate. With the gate valve open, the H_2 was pumped from the chamber via the orifice, and the steady-state pressures from both ion gages were recorded. The gate valve was then closed, and the rate of rise of the pressure in the chamber for this same in-flow rate was noted. This procedure was repeated with increasing H_2 flows until all scale ranges of the ion gages had been covered, with at least three data points on each scale.

The accumulated data were used in the following analysis to determine the gage sensitivity factors and the conductance of the orifice. Although the conductance of the orifice could be calculated, it was also measured experimentally to check the consistency of the equations, the applicability of kinetic theory, and the gage calibrations. The calculated value of the H_2 conductance using the Clausing factor (Ref. 7) was 141.5 ℓ/sec. The experimentally determined value was 143 ℓ/sec with a scatter of less than 5 percent. This agreement indicates that the experimental error in calibration does not exceed 5 percent.

4.2.1 Gage Calibration (Ion Gages)

From the ideal gas law

$$P \frac{dV}{dt} + V \frac{dP}{dt} = \frac{dn}{dt} RT$$

The gas flowing into the chamber may be considered as the sum of that through the leak Q_1 plus an outgassing load. Therefore,

$$P \frac{dV}{dt} + V \frac{dP}{dt} = Q_i + \xi \tag{1}$$

With the main gate valve closed, $\frac{dV}{dt} = 0$ and

$$\frac{dP}{dt} = \frac{Q_i + \xi}{V}$$

Assuming a constant outgassing rate it can be shown that

$$\sigma_{on} \dot{P}_{on} = \sigma_{cn} \dot{P}_{cn} = \frac{P_f k + \xi}{V} \tag{2}$$

where subscript cn refers to the c gage on the n scale and on refers to the o gage on the n scale.

Thus,

$$\frac{\dot{P}_{on}}{\dot{P}_{cn}} = \frac{\sigma_{cn}}{\sigma_{on}} \tag{3}$$

and a ratio of gage factors is obtained. From Eq. (2)

$$\dot{P}_{cn} = \frac{k}{\sigma_{cn} V} P_f + \frac{\xi}{\sigma_{cn} V} \tag{4}$$

Therefore, plotting $\dot{P}_{cn}$ versus P_f yields a straight line when outgassing is either constant or negligible. The volume V was determined during assembly of the chamber by measuring components and calculating the resultant volume. The values of σ_{cn} were determined by the slope of the straight line from Eq. (4), and σ_{on} was calculated from Eq. (3).

4.2.2 Orifice Calibration

Determination of the conductance of the orifice was made using the steady-state pressures. Since $\frac{dp}{dt} = 0$, then Eq. (1) reduces to

$$P \frac{dV}{dt} = Q_i + \xi \tag{5}$$

For this chamber, at the higher leak rates, $\xi \ll Q_1$, so that the outgassing may be ignored during calibration of the orifice. Thus,

$$P_c K - P_o K = P_f k$$

where K is the orifice conductance

and $$K = \frac{P_f k}{P_c - P_o}$$

Using the calibration factors already determined for the gages,

$$K = \frac{P_f k}{\sigma_{cn} P_{cn} - \sigma_{on} P_{on}}$$

Rewriting this expressing

$$K = \frac{P_f k}{\sigma_{cn} P_{cn} \left(1 - \frac{\sigma_{on} P_{on}}{\sigma_{cn} P_{cn}}\right)}$$

Over the range of flow rates used in these experiments, the ratio $\frac{\sigma_{on} \rho_{on}}{\sigma_{cn} \rho_{cn}}$ was found to be a constant. Therefore, we may define a K effective as

$$K_{eff} = K \left(1 - \frac{\sigma_{on} P_{on}}{\sigma_{cn} P_{cn}}\right) = \frac{P_f k}{\sigma_{cn} P_{cn}}$$

4.2.3 Calibration of Mass Spectrometer

The mass spectrometer was tested for linearity by closing off the diffusion pump and admitting H_2 to the chamber at a known rate. The resulting rate of rise of pressure as recorded by the mass spectrometer was linear over the pressure range to be used in these experiments (10^{-8} to 10^{-5} torr). The mass spectrometer was calibrated by flowing the H_2 into the chamber at a known rate with the diffusion pumping system removing the gas through the orifice. A record of the flow rates was plotted versus the equilibrium chamber pressures as recorded by the mass spectrometer. These data were obtained before each experimental run and constituted the calibration for the mass spectrometer.

4.2.4 Calculation of Pumping Speeds

Since the effective conductance of the orifice was known, it was not necessary to calculate a gage factor per se for the mass spectrometer in order to calculate pumping speeds of the cryodeposit. During the calibration, we may express the equilibrium conditions as:

$$P_{f_1} k_1 = \sigma_{ms} P_{ms_1} K_{eff}$$

Whereas during the pumping runs made with the diffusion pump valved off, the equilibrium condition may be written as

$$P_{f_2} k_2 = \sigma_{ms} P_{ms_2} S$$

where S is the pumping speed of the cryodeposit.

Therefore,

$$\frac{P_{f_1} k_1}{P_{f_2} k_2} = \frac{\sigma_{ms} P_{ms_1} K_{eff}}{\sigma_{ms} P_{ms_2} S}$$

and

$$S = \frac{P_{ms_1}}{P_{f_1}} \cdot \frac{P_{f_2}}{P_{ms_2}} \cdot \frac{k_2 K_{eff}}{k_1}$$

SECTION V
RESULTS

The H_2 partial pressure was monitored with a magnetic deflection-type mass spectrometer. This particular instrument is capable of reading partial pressures on the order of 5×10^{-10} torr. However, with no H_2 being admitted to the chamber, a H_2 background peak of 5×10^{-8} torr was observed. This peak was insensitive to pumping changes from 143 ℓ/sec (calibration orifice) to 28,000 ℓ/sec (12°K CO_2 cryodeposit) in the chamber. In calibrating the instrument, this background shows up as a zero shift in an otherwise linear calibration. It was, therefore, assumed that if this base peak represented a true H_2 gas partial pressure, it was being produced in the mass spectrometer head itself. The cell pressure was monitored by a Bayard-Alpert-type ion gage which indicated a pressure of 2×10^{-9} torr in the test chamber. Because of this masking effect of the actual base pressure in the cell, the "capacity" of a particular CO_2 cryodeposit was chosen as the quantity of H_2 required to raise the chamber partial pressure above 5×10^{-7} torr and thus be readily observable by the mass spectrometer. This definition is somewhat arbitrary but is necessary to allow us to compare the effects of temperature and thickness upon the pumping ability of the cryodeposit.

5.1 EFFECTS OF CRYODEPOSIT THICKNESS

The experimental results are divided into two groups: thin and thick deposits.

5.1.1 Thin Deposits

These deposits consisted of about 30 torr-ℓ of CO_2 which, assuming the bulk density of the cryodeposit as 1.5 gm/cc, represents a 5×10^{-5} cm layer. In each case, these deposits were made after the surface had reached the operating temperature chosen for the particular test run. At no time did the cell pressure rise above 10^{-4} torr during deposition of the cryolayer.

5.1.2 Thick Deposits

These deposits consisted of about 500 torr-ℓ of CO_2 which represents a layer about 1μ thick. The thickness of the CO_2 cryodeposit had no noticeable effect on the initial pumping speed of the H_2 at any of the temperatures tested. The capacity of the cryodeposit, however, seems to be a direct function of the quantity of the deposit over the range of thicknesses investigated (Fig. 3). Several deposits of CO_2 were left for periods of up to 1 hr before pumping runs were made to see if any tempering effects were noticeable, but none were found.

5.2 EFFECTS OF THE TEMPERATURE OF THE CRYODEPOSIT

Three temperatures were chosen for investigation: 20, 16, and 12°K. The radiation load in all cases, except one, was 300°K. The one result with a 77°K radiation load is noted separately. No pumping was observed for a cryodeposit at 25°K.

As can be seen in Table I, the most notable effect of the temperature is reflected in the capacity of the cryodeposit. A plot of the ratio of CO_2

TABLE I
RATIO OF CO_2/H_2 FOR VARIOUS TEMPERATURES

Temperature of Cryodeposit, °K	Amount CO_2 Deposited, torr-ℓ	Amount H_2 to Reach "Capacity", torr-ℓ	Ratio CO_2/H_2
20	30.3	0.06	500
	30.3	0.10	300
	630.0	2.04	309
16	30	0.63	47.5
	30	0.63	47.5
	514	9.0	57.0
12	30	3.75	8.0
	40	5.05	7.9
	495	58.0	8.5
for 20°K cryodeposit and 77°K shroud			
	495	9.0	55.0

to H_2 versus temperature (Fig. 4) indicates the order of magnitude improvement in the capacity as the temperature is lowered. The pumping speed of the cryodeposit shows some improvement with decreasing temperature. Average pumping speeds for 300°K H_2 were 14 ℓ/sec-cm^2 for 20°K cryodeposits, 19 ℓ/sec-cm^2 for 16°K cryodeposits, and 28 ℓ/sec-cm^2 for 12°K cryodeposits. These values are for H_2 addition rates on the order of 1 x 10^{-3} torr-ℓ/sec with H_2 partial pressures in the 10^{-8} torr range. A pressure dependence of the pumping speed as reported by Busol et al. (Ref. 4) was confirmed for the 20°K cryodeposits (Table II).

TABLE II
PUMPING SPEED OF H_2 VERSUS TEMPERATURE OF CO_2

Temperature of Deposit, °K	Flow Rate of H_2, torr-ℓ/sec	H_2 Partial Pressure during Pumping, torr	Pumping Speed, 1/sec-cm^2
Data taken September 23, 1966			
12.0	1.0 x 10^{-3}	3.52 x 10^{-8}	28.6
	6.0 x 10^{-3}	2.14 x 10^{-7}	28.4
	1.2 x 10^{-2}	4.32 x 10^{-7}	28.2
	3.5 x 10^{-2}	1.27 x 10^{-6}	27.9
	7.05 x 10^{-1}	2.51 x 10^{-6}	28.3
	1.06 x 10^{-1}	3.82 x 10^{-6}	28.1
	1.42 x 10^{-1}	5.1 x 10^{-6}	28.2
Data taken October 3, 1966			
16.0	1.0 x 10^{-3}	5.27 x 10^{-8}	19.2
	2.0 x 10^{-3}	1.11 x 10^{-7}	18.2
	6.0 x 10^{-3}	3.30 x 10^{-7}	18.4
	1.2 x 10^{-2}	7.81 x 10^{-7}	16.5
	2.0 x 10^{-2}	1.42 x 10^{-6}	14.3
Data taken September 22, 1966			
20.0	1.0 x 10^{-3}	6.95 x 10^{-8}	14.6
	2.0 x 10^{-3}	1.48 x 10^{-7}	13.7
	6.0 x 10^{-3}	1.44 x 10^{-6}	4.2
	1.2 x 10^{-2}	3.75 x 10^{-6}	3.2
	2.0 x 10^{-2}	8.4 x 10^{-5}	0.24
Data taken October 4, 1966		(Pressure and Pumping Speed Converted to 300°K)	
20.0 (77°K Shroud)	1.0 x 10^{-3}	3.12 x 10^{-8}	31.8
	2.0 x 10^{-3}	7.62 x 10^{-7}	26.6
	6.0 x 10^{-3}	3.24 x 10^{-6}	18.4
	1.2 x 10^{-2}	7.3 x 10^{-6}	16.4
	2.0 x 10^{-2}	1.26 x 10^{-6}	15.6

For these deposits, as the H_2 inflow was increased, the pumping speed started to deteriorate. However, if the H_2 flow was interrupted and then

restarted after the H_2 partial pressure had dropped to its base level, the pumping speed recovered for a short time before again starting to deteriorate.

For the 16°K cryodeposits, this deterioration of the pumping speed was not so pronounced, and recovery after an interruption was much faster. With the 12°K cryodeposits, no deterioration in pumping speed for H_2 flows up to 0.14 torr-ℓ/sec (H_2 partial pressure of 5×10^{-6} torr) was noted. A summary of pumping speed versus H_2 partial pressure is shown in Fig. 5.

The 20°K cryodeposit, surrounded by a 77°K radiation shield, showed a marked increase in initial pumping speed. However, the shape of a plot of the deterioration of pumping speed of this deposit versus H_2 partial pressure shows a marked resemblance to that of the 20°K cryodeposit with 300°K radiation (Fig. 5).

5.3 CONTAMINATION OF CRYODEPOSIT BY N_2

In this test, 495 torr-ℓ of CO_2 were predeposited and cooled to 12°K. Hydrogen was admitted to the cell at a flow rate of 2.1×10^{-2} torr-ℓ/sec. The initial pumping speed was 28.0 ℓ/sec-cm^2 which agrees with previous runs. Figure 6 shows a plot of the H_2 partial pressure as indicated by the mass spectrometer versus time as N_2 was admitted at different rates. Previous pumping runs with this thickness cryodeposit and the same H_2 inbleed rate showed no deterioration in pumping speed over a similar time period. A plot of pumping speed/cm^2 versus N_2 added/cm^2 pumping surface indicates a near logarithmic dependence as indicated in Fig. 7. A plot of rate of deterioration in pumping speed versus rate of N_2 addition is shown in Fig. 8 indicating a linear relationship.

SECTION VI
DISCUSSION

The data reported from these investigations cover a wide range of variables, and although no specific answers may be given from such a survey, several suggestions may be made concerning the mechanics of H_2 sorption by the cryodeposits. From the variation of thickness data, it would seem that within the range of these tests the complete cryodeposit is active in the sorption process at all the temperatures. An analysis of the pumping by different temperature cryodeposits indicates that the sorption process might be considered in two parts:

1. Impingement of H_2 molecules at the surface of the cryodeposit results in surface capture. For a fixed quantity of H_2 added to

the system, one would thus expect an equilibrium to be established where for a specific concentration of H_2 molecules within this surface, the re-evaporation rate would match the condensation rate. At this point the pumping would stop. However, coupled with this process there is:

2. A diffusion of H_2 molecules within the cryodeposit matrix from the region of high concentration at the surface. The rate constant for this diffusion is evidently strongly dependent upon the cryodeposit temperature.

This model will explain the pressure dependence of the pumping speed measurements made on 20°K cryodeposits and account for the recovery in pumping speed after a brief pause in H_2 additions. Also, the data presented in Fig. 5 for the pumping speed of a 20°K deposit with a 77°K shroud indicate that whereas the surface capture is improved by reducing the radiation load, the pumping speed is still limited by the inability of the H_2 molecules to diffuse into the cryodeposit matrix quickly enough.

It might be noted that the data presented in Fig. 5 should be accepted as indicating a trend rather than presenting absolute values. Since there is a correlation between the pumping speed at the surface and the relative saturation of the substrate, absolute values should be taken with a fresh cryodeposit for each data point. Although different cryodeposits were used for each temperature range shown in these data, pumping speed measurements were made in succession as the H_2 inflow rate was increased stepwise. These cryodeposits were above 1 μ thick. However, using thick layers of CO_2 reduces but does not eliminate the effect of H_2 sorbed in determining the previous data point.

An apparent logarithmic dependence of the ratio of quantities of CO_2 predeposited to H_2 required to saturate to capacity versus temperature is shown in Fig. 4. The limited scatter of these data warrants a more refined investigation of the effects of the cryodeposit's capacity as a function of its temperature. Investigation over a wider range of cryodeposit thicknesses at intermediate temperatures would help to better define this relationship.

The pumping speeds indicated in Fig. 7 show the adverse effects of N_2 condensing on the CO_2. The rapid equilibrium established when the N_2 flow was interrupted (as shown in Fig. 6) would indicate that the N_2 is confined to the surface rather than diffusing into the cryodeposit. A near logarithmic dependence between pumping speed and quantity of N_2 deposited was not expected. The data thus indicate that the poisoning does

not consist of a simple blocking of condensation sites, but rather acts as a permeable barrier. One would expect that with increasing thickness of this barrier, there would be a gradual transition from the pumping speed of H_2 on CO_2 cryodeposit to that of H_2 on N_2 cryodeposit.

SECTION VII
SUMMARY

Carbon dioxide cryodeposits may be used as an effective method of cryopumping H_2. The 12°K cryodeposits yielded pumping speeds of 28 ℓ/sec-cm^2 with no pressure dependence up to 5 x 10^{-6} torr. The 16°K cryodeposits yielded pumping speeds of 19 ℓ/sec-cm^2 with a drop in pumping speed at pressures above 5 x 10^{-7} torr, and 20°K cryodeposits yielded pumping speeds of 14 ℓ/sec-cm^2 with a drop in pumping speed at pressures above 5 x 10^{-8} torr.

The capacity of the cryodeposits is a direct function of its thickness within the range investigated and increases logarithmically as its temperature is lowered.

No pumping was observed with the cryodeposit above 25°K.

The cryodeposit is readily contaminated with N_2, and use of this system to pump mixtures of N_2 and H_2 would require shielding by 20°K baffles to remove the N_2 before it reached the CO_2 surface. Such shields would also reduce the radiation load and thus improve the pumping speed of the cryodeposit; however, this gain might be offset by losses caused by the limiting conductance of the baffle.

REFERENCES

1. Chubb, J. N. and Pollard, I. E. "Experimental Studies of Hydrogen Condensation Onto Liquid Helium Cooled Surfaces." Vacuum, Vol. 15, No. 10, October 1965, p. 491.

2. Haygood, J. D. and Dawbarn, R. "Helium Pumping by 4.2°K Cryodeposits." AEDC-TR-66-204 (AD645511), January 1967.

3. Southerlan, R. E. "10 to 22°K Cryosorption of Helium on Molecular Sieve 5A and Hydrogen on Condensed Vapors." AEDC-TR-65-49 (AD463339), May 1965.

4. Busol, F. I. and Yuferov, V. B. "New Method of Pumping Hydrogen." Soviet Physics - Technical Physics, Vol. 11, No. 1, July 1966, p. 125.

5. Stern, S. A., Hemstreet, R. A., and Ruttenbur, D. M. "Cryosorption Pumping of Hydrogen at 20°K. Development and Performance of Cryosorption Panels." Journal of Vacuum Science and Technology, Vol. 3, No. 3, May/June 1966, p. 99.

6. Matthews, A. J. "Evaluation of Porous Materials as Molecular Leaks." AEDC-TDR-64-94 (AD602922), July 1964.

7. Dushman, S. Scientific Foundations of Vacuum Technique. J. M. Lafferty (ed.), John Wiley and Sons, Inc., New York, 1949 (2nd Ed.)

APPENDIX
ILLUSTRATIONS

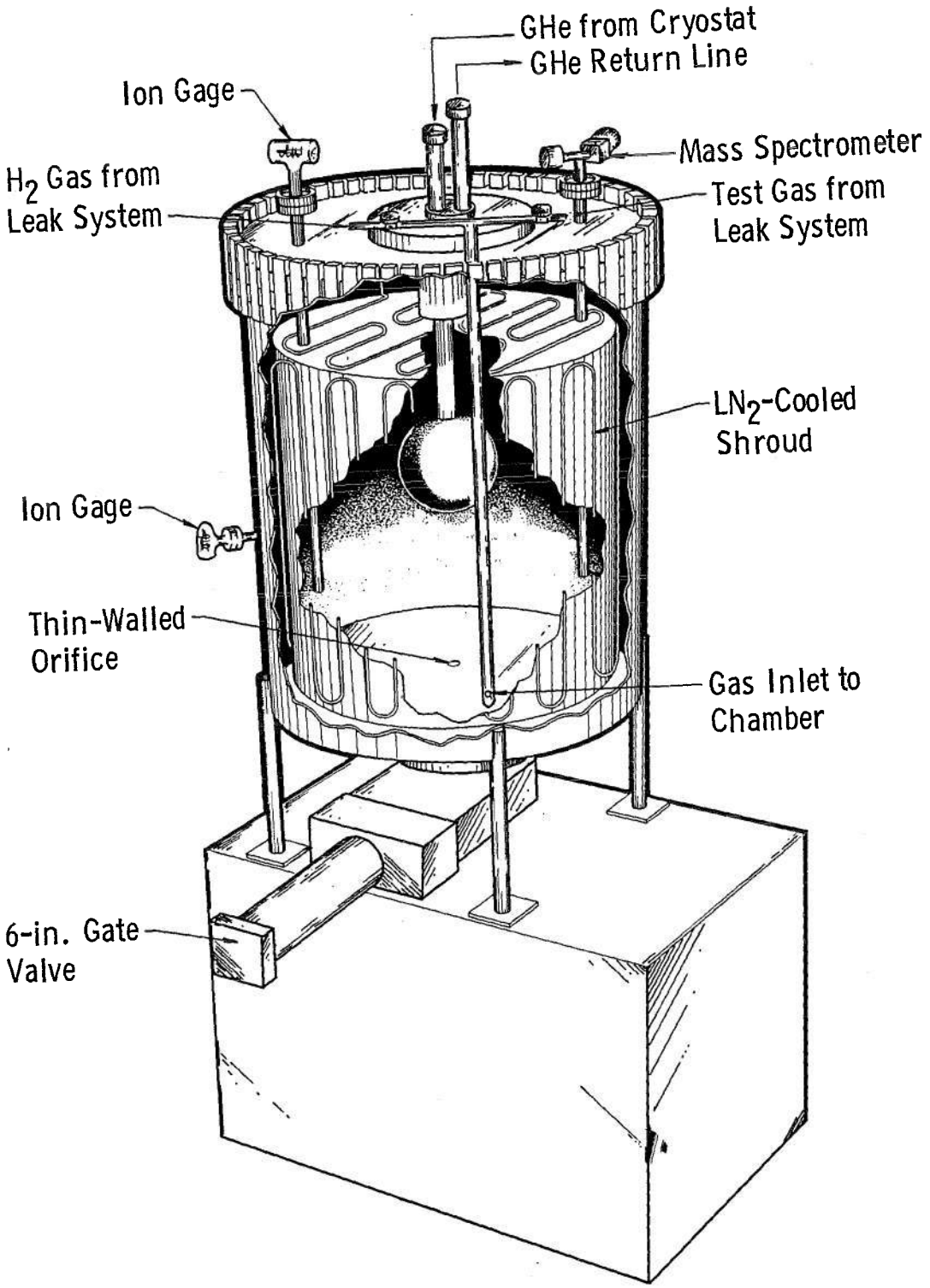

Fig. 1 UHV Chamber

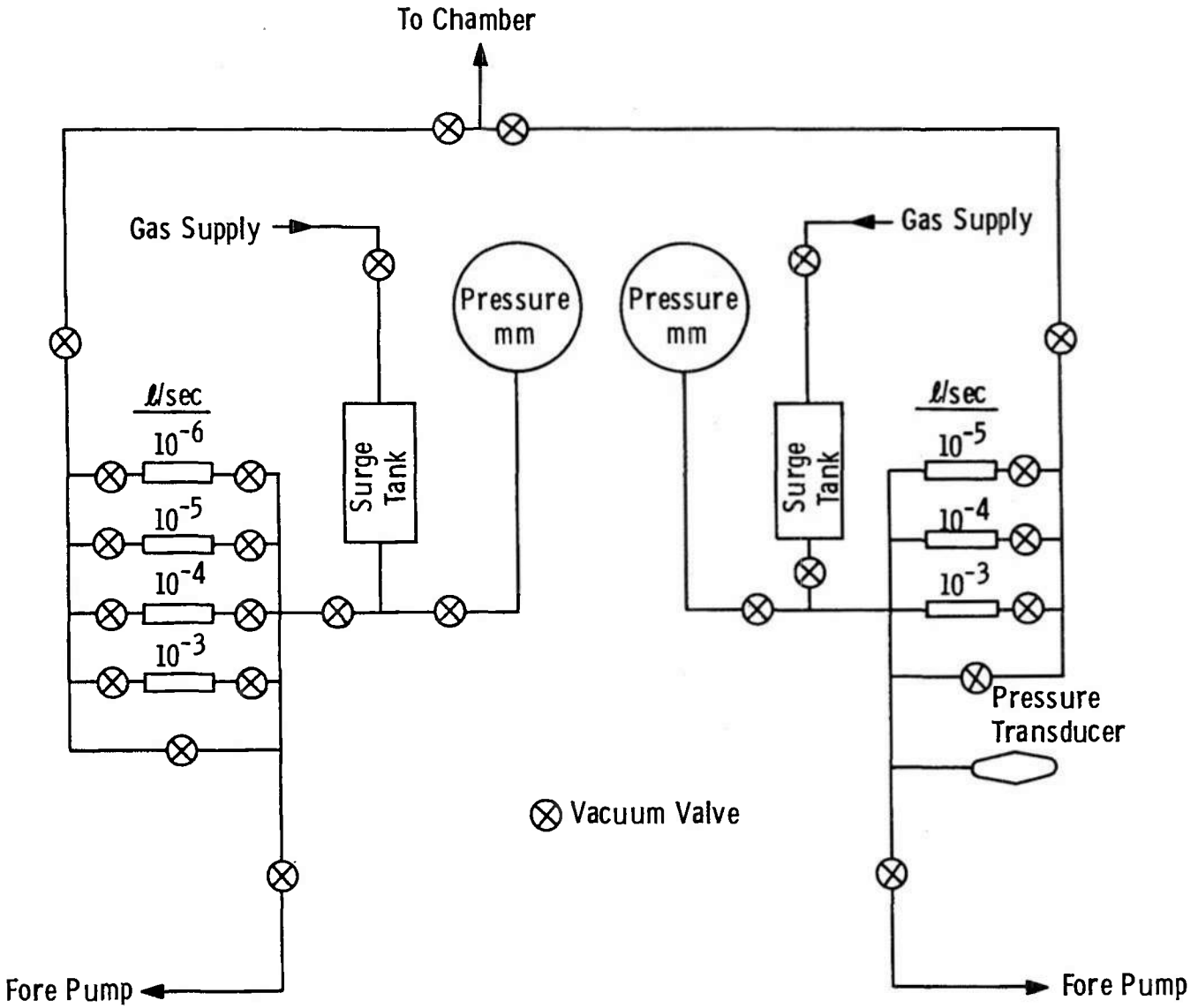

Fig. 2 Gas Addition System

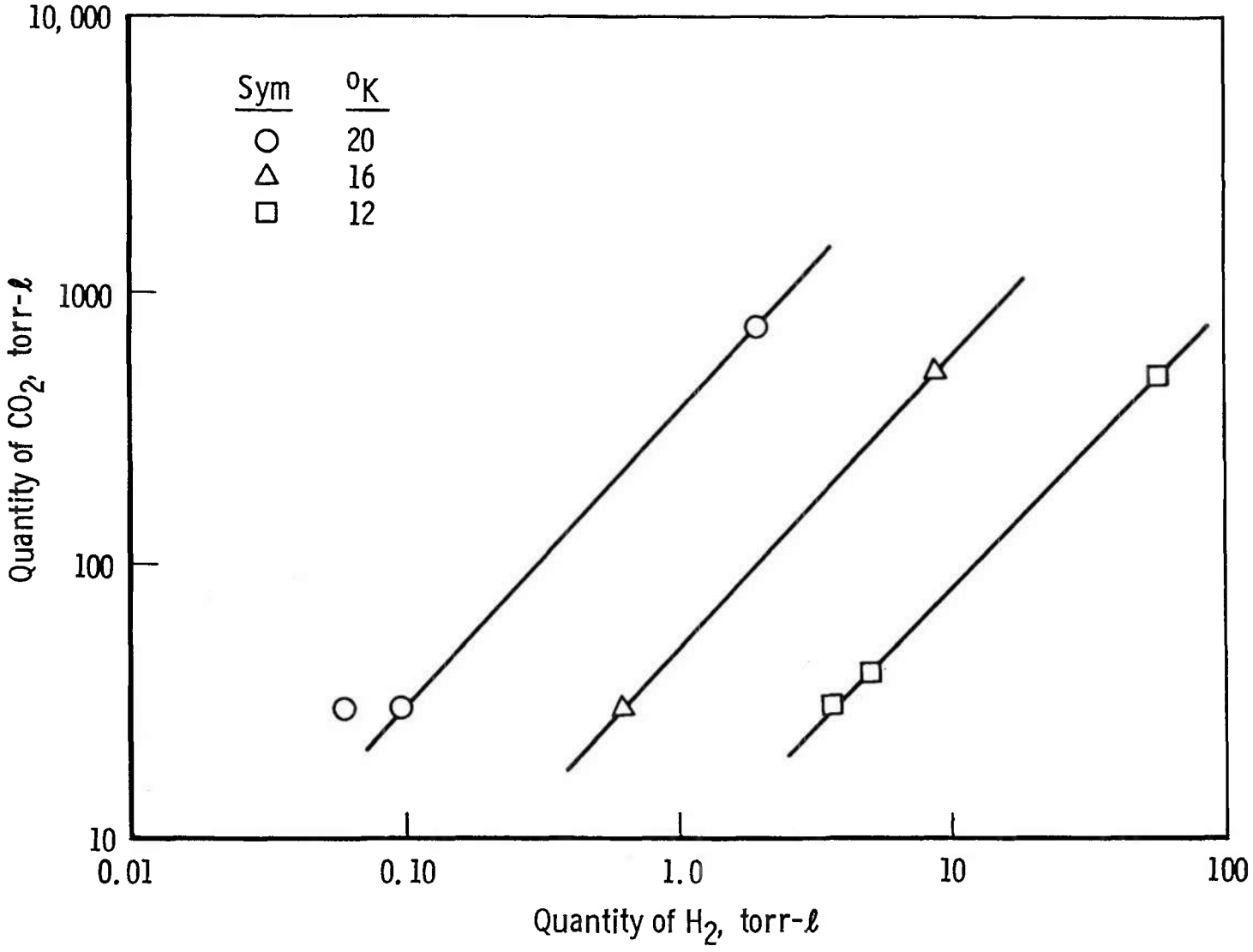

Fig. 3 Quantity of CO_2 Added versus H_2 Required to Reach Capacity

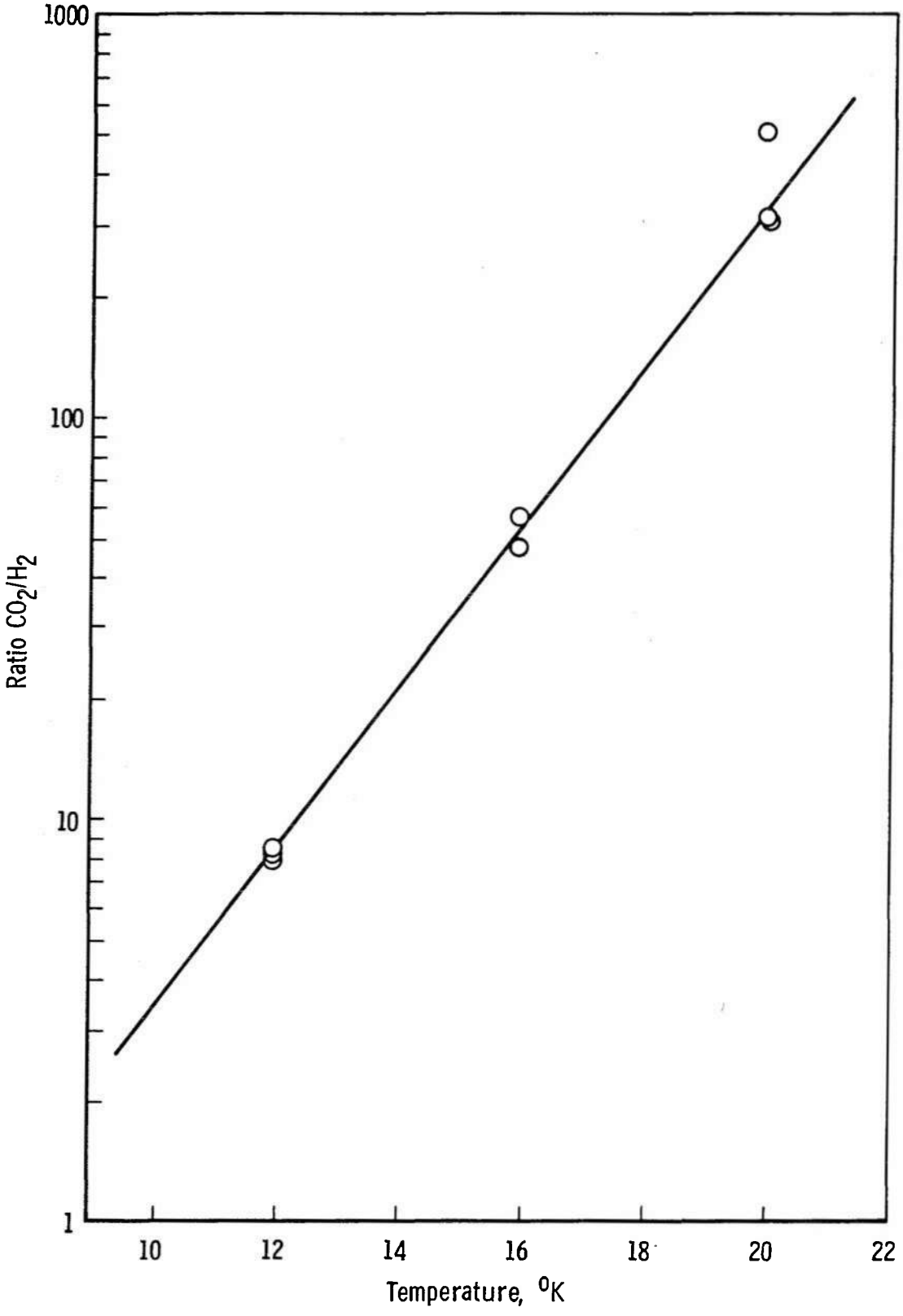

Fig. 4 Ratio of CO_2/H_2 (from Fig. 3) Plotted against Temperature

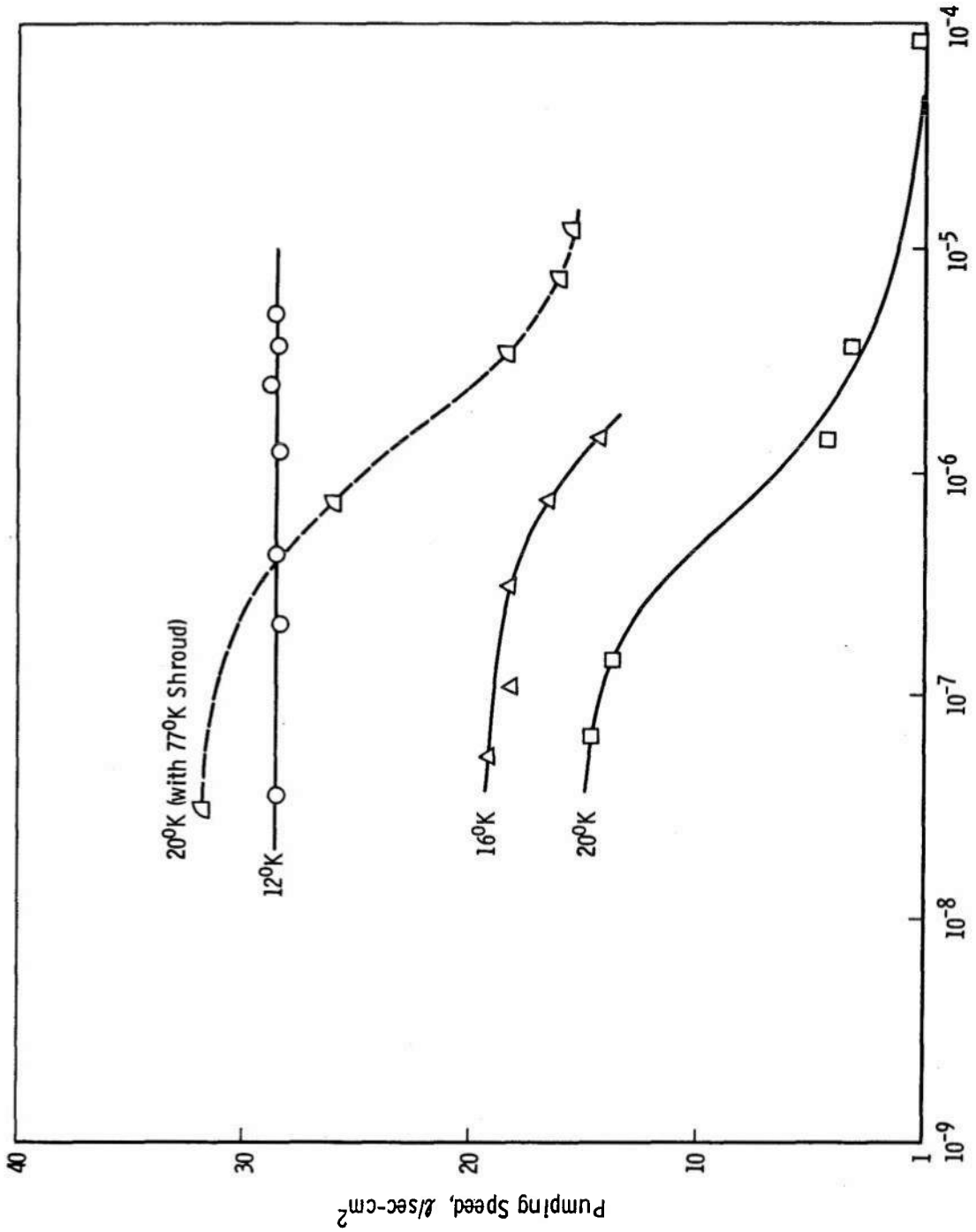

Fig. 5 Pressure Dependence of Pumping Speed

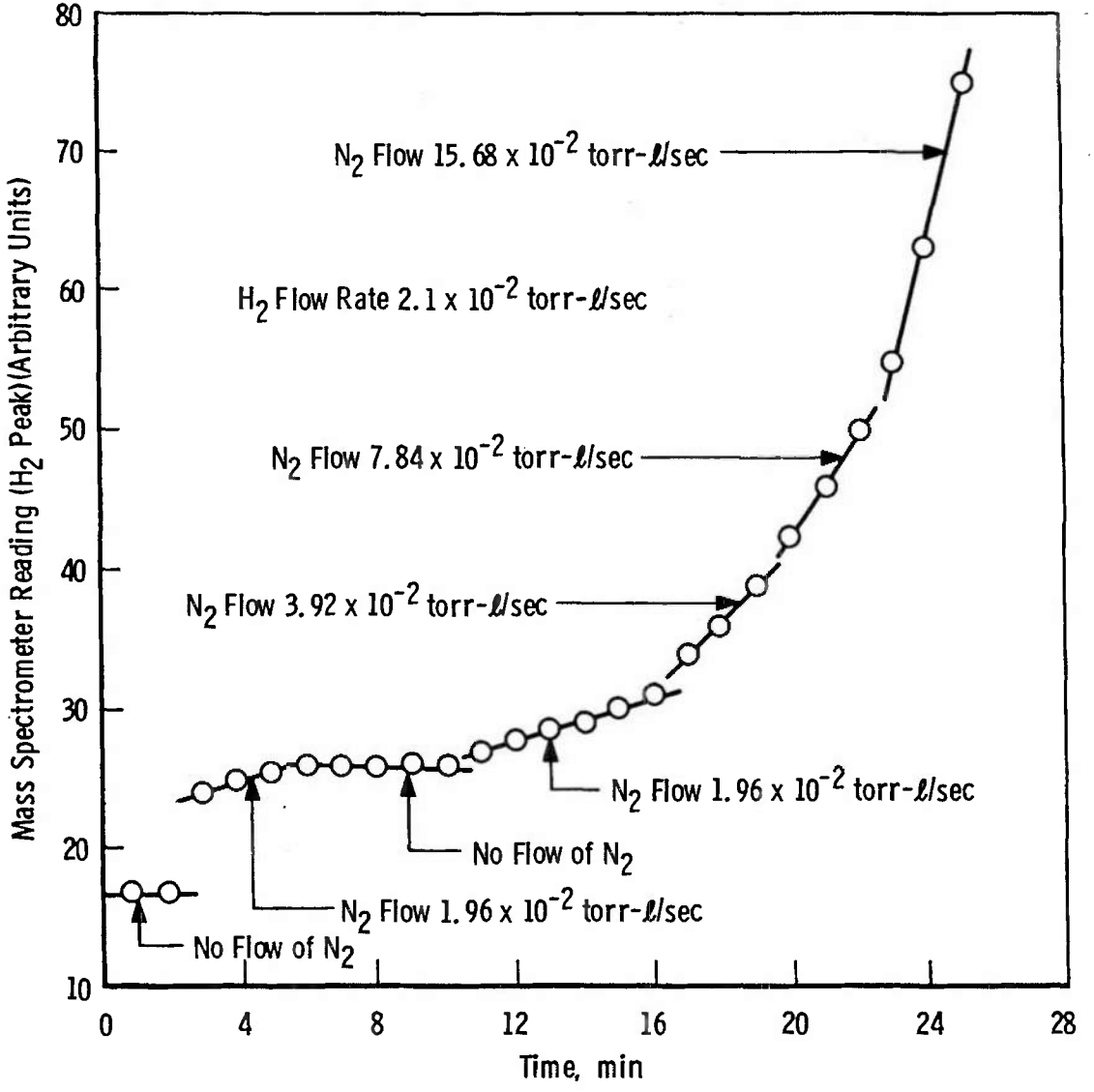

Fig. 6 Mass Spectrometer Trace during Poisoning of CO_2 Surface by N_2

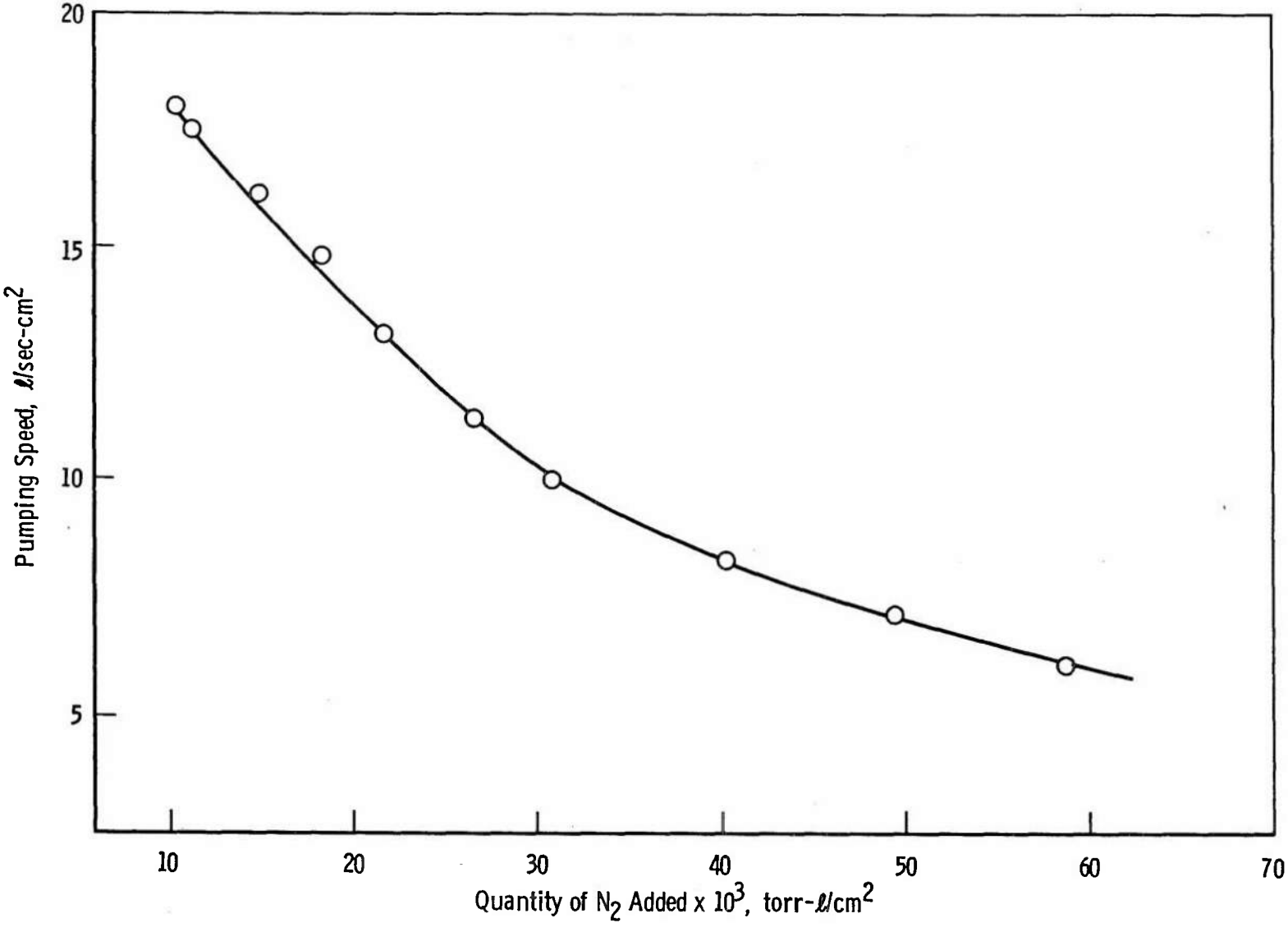

Fig. 7 Pumping Speed of Cryodeposit during Poisoning

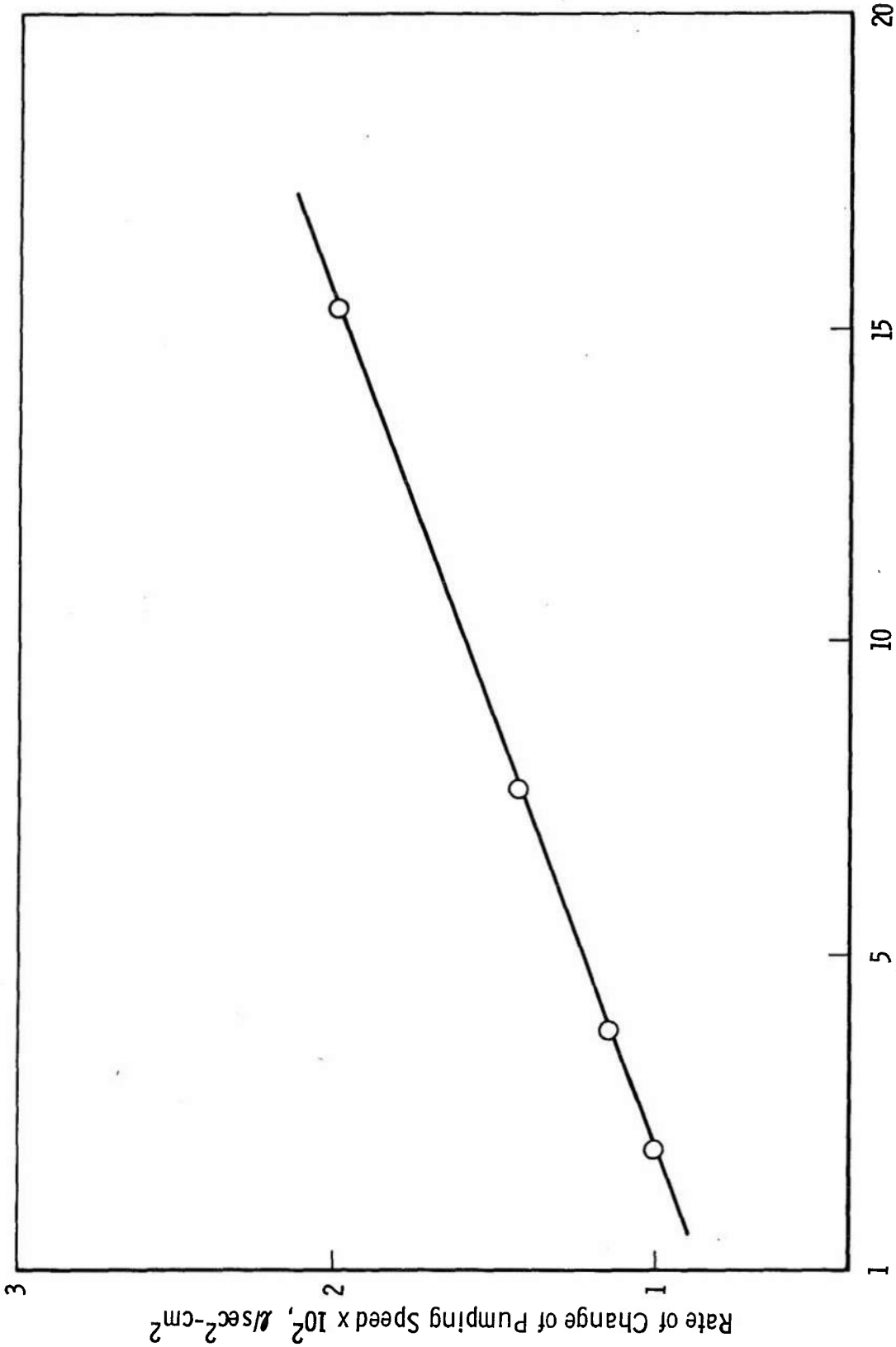

Fig. 8 Rate of Deterioration of Pumping Speed versus Rate of N_2 Addition

Security Classification

DOCUMENT CONTROL DATA - R&D

(Security classification of title, body of abstract and indexing annotation must be entered when the overall report is classified)

1. ORIGINATING ACTIVITY *(Corporate author)* Arnold Engineering Development Center ARO, Inc., Operating Contractor Arnold Air Force Station, Tennessee	2a. REPORT SECURITY CLASSIFICATION UNCLASSIFIED 2b. GROUP N/A

3. REPORT TITLE

CRYOSORPTION OF HYDROGEN BY 12-20°K CARBON DIOXIDE CRYODEPOSITS

4. DESCRIPTIVE NOTES *(Type of report and inclusive dates)*

Final Report September to October 1966

5. AUTHOR(S) *(Last name, first name, initial)*

R. Dawbarn, ARO, Inc.

6. REPORT DATE	7a. TOTAL NO. OF PAGES	7b. NO. OF REFS
July 1967	30	7

8a. CONTRACT OR GRANT NO.	9a. ORIGINATOR'S REPORT NUMBER(S)
AF 40(600)-1200 b. PROJECT NO. c. Program Element 65402234 d.	AEDC-TR-67-125 9b. OTHER REPORT NO(S) *(Any other numbers that may be assigned this report)* N/A

10. AVAILABILITY/LIMITATION NOTICES

This document has been approved for public release and sale; its distribution is unlimited.

11. SUPPLEMENTARY NOTES	12. SPONSORING MILITARY ACTIVITY
Available in DDC	Arnold Engineering Development Center Air Force Systems Command Arnold Air Force Station, Tennessee

13. ABSTRACT

Carbon dioxide cryodeposits were investigated to determine their ability to sorb H_2. Various thickness from 5×10^{-5} to 1×10^{-3} cm were used, at temperatures of 12, 16, and 20°K. Pumping speeds of 28, 19, and 14 ℓ/sec-cm^2 were measured for the respective temperatures. An arbitrary "Capacity" of the CO_2 cryodeposit for H_2 was defined. Within the limits of the experimental parameters varied, this capacity was found to be a direct function of the thickness of the cryodeposit and increased logarithmically as the temperature was lowered. No cryopumping of H_2 was observed with cryodeposits above 25°K. The CO_2 cryodeposits were readily contaminated by N_2, and the H_2 pumping speed dropped when N_2 was flowed in simultaneously with the H_2.

DD FORM 1 JAN 64 1473

Security Classification

Security Classification

14. KEY WORDS	LINK A		LINK B		LINK C	
	ROLE	WT	ROLE	WT	ROLE	WT
1 cryosorption hydrogen 2 carbon dioxide cryodeposits 3 "						

3. Hydrogen -- Sorption

15-2.

Security Classification